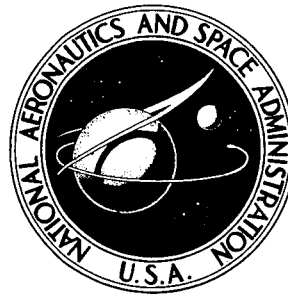


148

**NASA TECHNICAL
MEMORANDUM**



NASA TM X-2783

NASA TM X-2783

0311237

(NASA-TM-X-2783) STEADY-STATE HOT-ION
PLASMA PRODUCED BY CROSSED ELECTRIC AND
MAGNETIC FIELDS (NASA) 16 p HC \$3.00

N73-21613

CSSL 20I

Unclas
68831

H1/25

**STEADY-STATE HOT-ION PLASMA
PRODUCED BY CROSSED ELECTRIC
AND MAGNETIC FIELDS**

by Donald R. Sigman and John J. Reinmann

Lewis Research Center

Cleveland, Ohio 44135

1. Report No. NASA TM X-2783	2. Government Accession No.	3. Recipient's Catalog No.	
4. Title and Subtitle STEADY-STATE HOT-ION PLASMA PRODUCED BY CROSSED ELECTRIC AND MAGNETIC FIELDS		5. Report Date April 1973	
		6. Performing Organization Code	
7. Author(s) Donald R. Sigman and John J. Reinmann		8. Performing Organization Report No. E-7303	
		10. Work Unit No. 503-10	
9. Performing Organization Name and Address Lewis Research Center National Aeronautics and Space Administration Cleveland, Ohio 44135		11. Contract or Grant No.	
		13. Type of Report and Period Covered Technical Memorandum	
12. Sponsoring Agency Name and Address National Aeronautics and Space Administration Washington, D.C. 20546		14. Sponsoring Agency Code	
15. Supplementary Notes			
16. Abstract <p>Results of initial diagnostics on the Lewis Research Center hot-ion-plasma source (HIP-1) are reported. The mirror-contained plasma was heated by applying a radial electric field similar to that used in the ORNL Burnout experiments. An electrostatic neutral particle analyzer was used to make a parametric study of ion energy distributions in both hydrogen and deuterium plasmas. Ion temperatures as high as 2 keV were measured in plasmas with electron densities greater than 10^{12} cm^{-3}. The performance of the device was found to be extremely sensitive to magnetic field. There are indications that ion-heating was reduced when the size of the Larmor orbit was larger than the region of strong radial electric field.</p>			
17. Key Words (Suggested by Author(s)) Plasma source Ion heating		18. Distribution Statement Unclassified - unlimited	
19. Security Classif. (of this report) Unclassified	20. Security Classif. (of this page) Unclassified	21. No. of Pages 16	22. Price* \$3.00

STEADY-STATE HOT-ION PLASMA PRODUCED BY CROSSED ELECTRIC AND MAGNETIC FIELDS

by Donald R. Sigman and John J. Reinmann

Lewis Research Center

SUMMARY

Results of initial diagnostics on the Lewis Research Center hot-ion-plasma source (HIP-1) are reported. The mirror-contained plasma was heated by applying a radial electric field similar to that used in the Oak Ridge National Laboratory (ORNL) Burnout experiments. An electrostatic neutral particle analyzer was used to make a parametric study of ion energy distributions in both hydrogen and deuterium plasmas. Ion temperatures as high as 2 keV were measured in plasmas with electron densities greater than 10^{12} cm^{-3} . The performance of the device was found to be extremely sensitive to magnetic field. There are indications that ion heating was reduced when the size of the Larmor orbit was larger than the region of strong radial electric field.

INTRODUCTION

This report describes the first experimental data obtained with the HIP-1 (hot-ion plasma) source at the NASA Lewis Research Center. In this facility, energy is coupled to the plasma by applying a radially inward dc electric field \mathcal{E} near the maximum field region of a magnetic mirror. The mutually perpendicular electric and magnetic fields cause the plasma to rotate (drift) in the azimuthal direction with a velocity $c\mathcal{E}/B_0$. (All symbols are defined in the appendix.) According to the theory of Hirose and Alexeff (ref. 1) an azimuthal current exists because of a drift velocity difference between ions and electrons. The combination of this current and a radial density gradient leads to the growth of electrostatic azimuthal waves at frequencies near the lower hybrid frequency, $\omega_{\text{LH}} = \omega_{\text{pi}} / \left[1 + (\omega_{\text{pe}}^2 / \omega_{\text{ce}}^2) \right]^{1/2}$. Hirose and Alexeff then postulate that ions are heated in planes perpendicular to the applied magnetic field by the high-frequency fields of the wave. A similar experiment, the Burnout (ref. 2) experiment at the Oak Ridge National Laboratory (ORNL), has yielded ion temperatures as high as 3 keV and particle densities greater than 10^{13} cm^{-3} .

DESCRIPTION OF EXPERIMENT

A schematic of the experimental apparatus is shown in figure 1. The maximum value of magnetic field at the midplane B_0 was 1.8 teslas and the mirror ratio was 1.58. The voltage available to be applied to the electrodes was 20 kilovolts. The gas feed was through the center of the cathode. The electrodes were identical to those used in the Burnout VI experiment at ORNL.

There are several modes of operation of the facility, depending on the background gas pressure. At low pressures (below 5×10^{-5} torr) a faint glow discharge exists, and the full 20 kilovolts of the power supply can be applied without arcing. However, less than 0.1 ampere is drawn. At higher pressures (above 2×10^{-4} torr), very high currents exist (4 to 6 A); but the voltage between the electrodes drops severely as a result of a ballast resistor in series with the plasma. At intermediate pressures of approximately 1×10^{-4} torr, a high-voltage (8 to 10 kV), intermediate-current (1 A) mode exists. Preliminary ion temperature measurements indicated the highest values for this mode, and consequently all the data presented hereinafter are at $p \approx 1 \times 10^{-4}$ torr.

The current-voltage characteristics for the intermediate-pressure mode are as follows: As the voltage between electrodes is first raised from zero, very little current flows. Then at about 2 to 4 kilovolts the current starts to rise rapidly until a nearly saturated value is reached. Further raising of the voltage then leads to only slightly higher currents. Finally, a limitation is reached on the voltage when an arc occurs between the electrodes. This arc overvoltage is found to be from 9 to 12 kilovolts, being higher for larger magnetic fields. The ballast resistor mentioned previously is used to limit the current when it first begins to rise rapidly.

Conditioning was also found to be an important factor in achieving the hot-ion mode previously described. Whenever the system has been open to atmosphere or just sitting overnight, the high-current mode prevails when the voltage is applied. It was assumed that this is caused by a pressure increase due to outgassing from the carbon electrodes as they heat up. After several runs, however, the outgassing either ceases or reaches a constant level and repeatable operation in the hot-ion mode is possible. Hydrogen seems to condition more rapidly than deuterium. The highest currents also occur in hydrogen (up to 1.2 A); whereas, the maximum achievable current in deuterium is about 0.8 ampere. Any attempt to raise the currents above these values by raising the gas flow rate always leads to the high-current mode.

DIAGNOSTICS

Most of the data herein come from two principal diagnostics: (1) the measurement of the energy spectrum of charge-exchange neutrals escaping the plasma and (2) the

measurement of the Doppler-broadened 486.1-nanometer β -line of hydrogen or deuterium.

Neutral Particle Energy Analyzer

A schematic of the neutral particle energy analyzer (NPEA) and its arrangement with respect to the plasma is shown in figure 2. The NPEA was a duplicate of the one described in reference 3, but with a different particle detector. After emerging from the plasma, the collimated beam of neutrals was ionized in the nitrogen gas cell. The energy distribution of the beam of positive ions was obtained by sweeping the voltage on the 90° electrostatic deflection plates. The detector was a Bendix model 306 magnetic electron multiplier (MEM). The current output of the MEM was fed into a Keithley model 417 picoammeter. The output of the picoammeter went to the y-input of an x-y recorder. The NPEA sampled, from along a chord of plasma, a region approximately 1 centimeter high (vertical) and 2.5 centimeters wide (parallel to the magnetic field). The NPEA apparatus was mounted so that the plasma could be scanned vertically by pivoting the beam line about the point located at the test section flange so designated in figure 2.

The ion energy distribution within the plasma was obtained from the energy distribution at the detector output in the following manner: The detector current is proportional to the product of several factors

$$I(E) \sim \sigma_{cx}(E) v \Delta n_E K_{GC} K_{EDP} K_D \quad (1)$$

where

$I(E)$	detector current originating from ions in plasma with energies between E and $E + \Delta E$
$\sigma_{cx}(E)$	charge exchange cross section between ions and molecular hydrogen
v	speed of ions with energy $E = 1/2 m_i v^2$
Δn_E	number of plasma ions per unit volume with energies between E and $E + \Delta E$
$K_{GC}(E)$	neutral-to-ion conversion efficiency of nitrogen gas cell
$K_{EDP}(E)$	energy resolution of electrostatic deflector plates
$K_D(E)$	secondary emission coefficient for plasma ions incident on MEM tungsten cathode

The charge exchange cross sections σ_{cx} were taken from reference 4. The gas cell conversion factors K_{GC} presented in reference 5 were used. The energy resolution of the electrostatic deflector plates K_{EDP} was proportional to $E/\Delta E$. Least known was the secondary emission coefficient K_{D} for plasma ions incident on the MEM's tungsten cathode. We assumed that K_{D} is proportional to E . The variation of Δn_{E} with energy depended on the energy distribution within the plasma. We assumed an isotropic distribution in velocity space which resulted in the following relation:

$$\Delta n_{\text{E}} \sim v^2 f\left(\frac{mv^2}{2}\right) \Delta v = \frac{v}{m} f\left(\frac{mv^2}{2}\right) \Delta\left(\frac{mv^2}{2}\right)$$

In terms of energy, Δn_{E} has the following proportionality:

$$\Delta n_{\text{E}} \sim \sqrt{E} f(E) \Delta E$$

Substituting these energy dependences into equation (1) yielded the energy distribution function $f(E)$ in the plasma

$$f(E) \sim \frac{I(E)}{\sigma_{\text{cx}}(E) E^3 K_{\text{GC}}(E)} \quad (2)$$

Doppler Broadening

To make the Doppler-broadening measurements we employed a simple two-slit collimator to view along a chord of the plasma, the line of sight being horizontal and perpendicular to the axial magnetic field. The light sampled came from a plasma region approximately 1 centimeter vertically by 7.5 centimeters axially, and vertical scans could be made to look along various chords. The spectra were taken with a Jarrell-Ash 0.5-meter Ebert spectrometer.

Other diagnostics used so far to take a cursory look at the plasma were 8-millimeter microwave interferometry for electron density, Langmuir probes for plasma potential, and relative intensity measurements of helium lines at 504.8 and 471.3 nanometers for electron temperature.

EXPERIMENTAL RESULTS

Neutral Particle Measurements

Figure 3 shows a comparison of the NPEA detector current as a function of energy for hydrogen and deuterium for a discharge with an applied voltage V_0 of 8 kilovolts and a B_0 of 1.35 teslas. These are typical spectra for almost all values of V_0 and B_0 for which the hot-ion mode exists. In deuterium, the peak was broader but the high-energy tail was always less relative to the peak than is the case for hydrogen.

Figure 4 shows reduced energy spectra $f(E)$ for the best achievable conditions of $V_0 = 10$ kilovolts and $B_0 = 1.8$ teslas. In reducing these data it was assumed that the charge exchange was between molecules and ions. We see that the temperatures indicated by the slope of the curves at high energies are 2 keV for hydrogen and 1 keV for deuterium. The two nearly identical curves for deuterium indicate that the shape of the spectrum is roughly the same whether one is viewing directly through the center of the plasma or along a chord passing 1.5 centimeters below the center. Figure 5 shows two of the curves from figure 4 replotted as a function of AE where A is 1 for hydrogen and 2 for deuterium. Equal values of AE correspond to equal values of the Larmor radius.

As one scans the plasma and looks at successive chords both above and below the centerline of the plasma, there is evident an asymmetry in the relative amplitudes of the spectra. This is caused by the fact that in a rotating (drifting) plasma there are more particles of a given energy moving toward the analyzer which are below the centerline than there are above the centerline. A reversal of the magnetic field direction reversed this asymmetry. It is unfortunate that this drift-related azimuthal variation in the velocity distribution makes it impossible to Abel-invert the data to determine the radial variation of the distribution function.

Figure 6 shows reduced data ($V_0 = 8$ kV, $B_0 = 1.35$ T) taken along a line of sight through the center of the plasma and also along a line of sight 1.5 centimeters below the center. The qualitative aspects are the same for hydrogen and deuterium. The curves for each gas have been normalized at 1 keV. One possible interpretation of these data is that the temperature of the plasma is peaked near the center; hence, the tail of the distribution is enhanced when sighting through the plasma center. This was not found to be the case for the same two sighting positions at $V_0 = 10$ kilovolts and $B_0 = 1.8$ teslas (fig. 4).

It also may be that the highest energy particles were carbon (or some other impurities). A momentum analyzer, now being built, will tell us whether species other than H (or D) contribute to the measured currents. One must realize that a clear interpretation of such data is difficult because (1) the effect of plasma drift on the distribution

changes with each new line of sight, and (2) the data presented are an integration along a chord of the plasma.

Figure 7(a) shows hydrogen raw data spectra with B_0 as a parameter and V_0 fixed at 8 kilovolts, while figure 7(b) has V_0 as a parameter and B_0 fixed at 1.8 teslas. Part of these data are then replotted in figures 7(c) and (d) as the ratio $I(E)/I(1.0 \text{ keV})$ as a function of B_0 and V_0 , respectively. An increase in this ratio means there is a higher fraction of the ions at high energies, and we interpret this as ion heating. The data show an apparent increase in ion heating with increases in B_0 and/or V_0 .

One can get an idea of the plasma diameter by cross plotting data at a given particle energy from spectra taken along various lines of sight. Figures 8(a) and (b) show such plots for both hydrogen and deuterium and for several energies. The mean plasma diameter was approximately 2 centimeters and was slightly larger for deuterium than for hydrogen. If it were possible to Abel-invert the data, the mean diameter would probably be slightly larger. The shift of the data peaks away from the centerline sighting position was again caused by the drift. For the higher energy particles, the Larmor orbits were large enough to cover a sizeable portion of the plasma. This tended to "smear out" the drift asymmetry.

Doppler Broadening

Figure 9 shows typical $H\beta$ spectra ($V_0 = 8 \text{ kV}$, $B_0 = 1.35 \text{ T}$) for sightings below, through, and above the centerline, respectively. The center of the broadened base, which comes from the fast charge exchange neutrals, shifts from below 486.1 nanometer to above as the line of sight is shifted upward. The maximum shift away from 486.1 nanometers is about 1.2 nanometers, which corresponds to a plasma drift velocity of 7.4×10^6 centimeters per second. Later we discuss measurements which indicate that the potential on centerline at the midplane was approximately 40 percent of that applied to the cathodes. Using this value, we calculated an average electric field in the previously discussed annular region between the electrodes of 3 kilovolts per centimeter. The cE/B drift velocity was then computed to be 2×10^7 centimeters per second, or about three times that measured by the shift. This is not necessarily inconsistent when one considers the fact that the lifetime of the excited states is of the order of 10^{-8} second. Thus, the hot neutral atoms may travel a significant distance across the plasma before radiating, making the origin of the light quite different from the position of the original ion. This effect will tend to reduce the measured drift.

When $G(\lambda)$ from figure 9 is plotted logarithmically as a function of $(\Delta\lambda)^2$ (where $(\Delta\lambda)^2 \sim E$), the broadened base part of these curves gives a straight line. The temperature related to the slope of this line is 0.35 keV for hydrogen. Raising the magnetic

field to 1.5 teslas raised this value to 0.40 keV. These non-Abel-inverted ion temperature values determined from the spectroscopic data probably represent a mean value for the whole plasma; whereas, the higher values determined from the tail of the NPEA data are either indicative of the peak temperatures or represent data for other species.

Figure 10 shows the peak of the $H\beta$ curves plotted as a function of sighting position ($V_0 = 8$ kV, $B_0 = 1.35$ T). The plasma diameter indicated here is the same as that derived from the neutral particle data (~ 2 cm).

Other Diagnostics

The beam of the microwave interferometer used to make electron density measurements was larger than the plasma diameter. This is certainly far from an ideal condition and would lead to a measured phase shift for the whole beam which is less than the phase shift of the portion of the beam which passed through the plasma. Thus, all we can say is that the mean density n_e of the plasma is greater than 10^{12} cm^{-3} .

Electron temperature T_e measurements using the helium line intensity ratio method were made only in hydrogen for $V_0 = 8$ kilovolts and $B_0 = 1.2$ teslas. The measured value for T_e was 12 eV. Since these are conditions of low power input to the plasma, it is probably safe to say that the electron temperature for the conditions discussed herein was greater than 12 eV.

A probe actuator was used to inject a Langmuir probe to the center of the plasma and out again in less than 0.1 second. At 4 and 6 kilovolts the probe measured potentials on axis of approximately 40 percent of the applied voltage. Under these conditions the probe became incandescent during the traverse. At 8 kilovolts the probe disintegrated. These measurements give further evidence that a large radial electric field exists in the midplane as well as at the mirror throats.

CONCLUDING REMARKS

Initial diagnostics on the HIP-1 hot-ion-plasma source revealed more than one mode of operation. Highest ion temperatures were observed in a mode where the total cathode-anode current was limited to approximately 1 ampere. Highest temperatures measured were about 2 keV in hydrogen and 1 keV in deuterium. Plasma heating was found to increase with applied voltage and/or dc magnetic field strength, being more sensitive to the magnetic field. Electron densities were greater than 10^{12} cm^{-3} . Evidence of plasma rotation was seen through asymmetries in radial scans of the neutral particle energies and the Doppler-broadened $H\beta$ line. Determination of the ion energy

distribution function was difficult because of the strong role played by ion drifts in determining the measured neutral particle energy spectrum.

Lewis Research Center,
National Aeronautics and Space Administration,
Cleveland, Ohio, February 7, 1973,
503-10.

APPENDIX - SYMBOLS

A	atomic number for ions
B_0	axial magnetic field at midplane
c	speed of light
E	ion or neutral particle energy
\mathcal{E}	radial electric field
f	plasma energy or velocity distribution function
G	spectrometer current
I	neutral particle analyzer detector current
K_D	neutral particle analyzer detector efficiency
K_{EDP}	electrostatic analyzer resolution
K_{GC}	gas stripping cell conversion efficiency
m_i	ion mass
n_e	electron density
p	background gas pressure
T_e	electron temperature
V_0	applied voltage between electrodes
v	ion or neutral velocity
λ	wavelength
σ_{cx}	charge exchange cross section for H (or D) ions on molecular H_2 (or D_2)
ω_{ce}	electron cyclotron frequency
ω_{LH}	lower hybrid frequency
ω_{pe}	electron plasma frequency
ω_{pi}	ion plasma frequency

REFERENCES

1. Hirose, A.; and Alexeff, I.: Electrostatic Instabilities Driven by Currents Perpendicular to an External Magnetic Field. Nucl. Fusion, vol. 12, no. 3, May 1972, pp. 315-323.
2. Anon.: Thermonuclear Division Annular Progress Report for Period Ending December 31, 1970. Rep. ORNL-4688, Oak Ridge National Lab., Aug. 1971, pp. 77-89.
3. Valckx, F. P. G.: Electrostatic Analyzer for the Detection of Fast Neutral Particles. NASA TT F-11458, 1968.
4. Berkner, Klaus H.; Pyle, Robert V.; and Stearns, J. Warren: Cross Sections for Electron Capture by 0.3 to 70 keV Deuterons in H_2 , H_2O , CO , CH_4 and CHF_{16} Gases. Rep. UCRL-18738, Univ. California Lawrence Radiation Lab., June 2, 1969.
5. Barnett, C. F.; and Ray, J. A.: A Calibrated Neutral Atom Spectrometer for Measuring Plasma Ion Temperatures in the 0.165- to 10-keV Energy Region. Nucl. Fusion, vol. 12, no. 1, Jan. 1972, pp. 65-72.

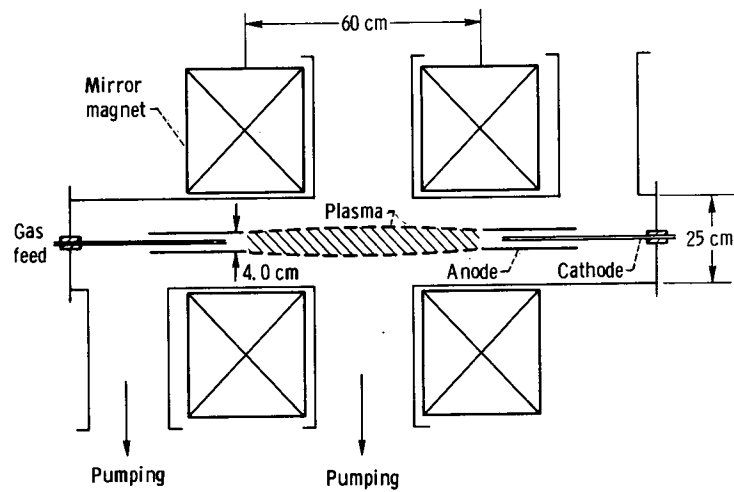


Figure 1. - Hot-ion-plasma (HIP-1) source.

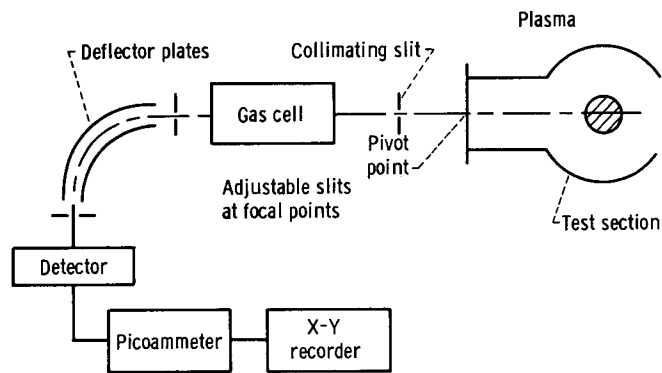


Figure 2. - Neutral particle energy analyzer.

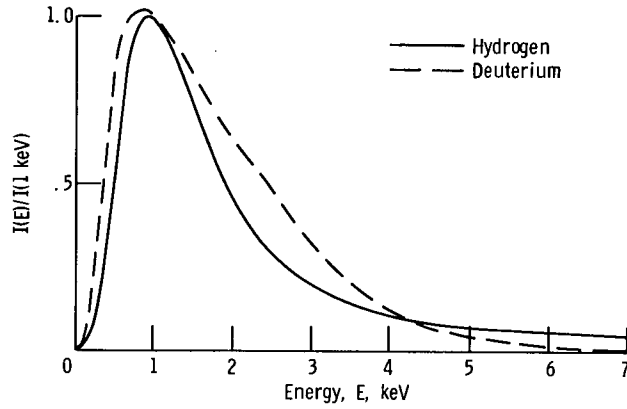


Figure 3. - Typical unreduced neutral particle energy spectra $I(E)$ as function of energy. Applied voltage between electrodes, 8 kilovolts; axial magnetic field at midplane, 1.35 teslas.

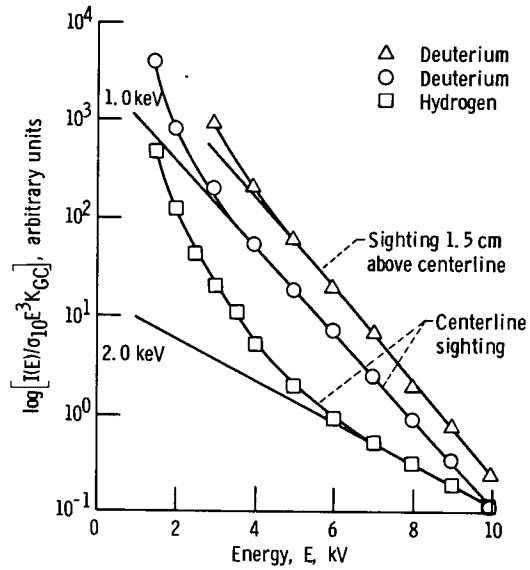


Figure 4. - Reduced energy spectra as function of energy for applied voltage between electrodes of 8 kilovolts and axial magnetic field at midplane of 1.8 teslas. $f(E) \sim I(E)/\sigma_{10}E^3K_{GC}$.

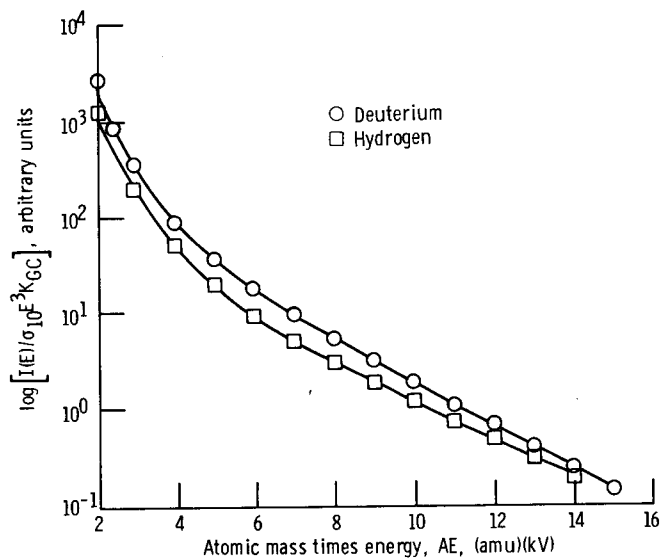


Figure 5. - Reduced energy spectra as function of AE (atomic number times energy) for applied voltage between electrodes of 8 kilovolts and axial magnetic field of 1.8 teslas. Centerline sighting.

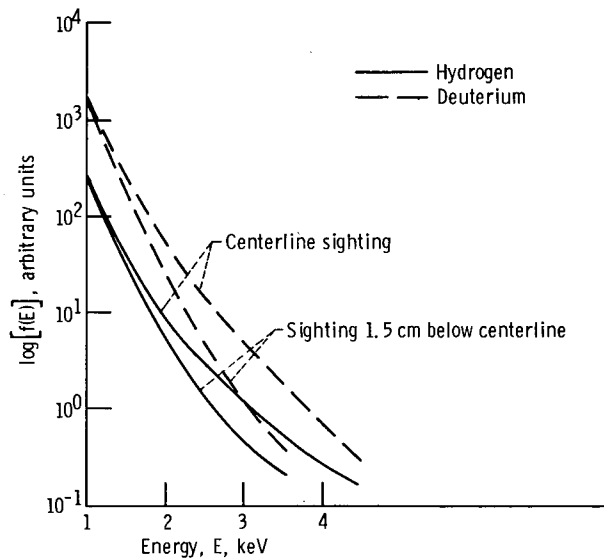


Figure 6. - Reduced energy spectra as function of energy for applied voltage between electrodes of 8 kilovolts and axial magnetic field at midplane of 1.35 teslas.

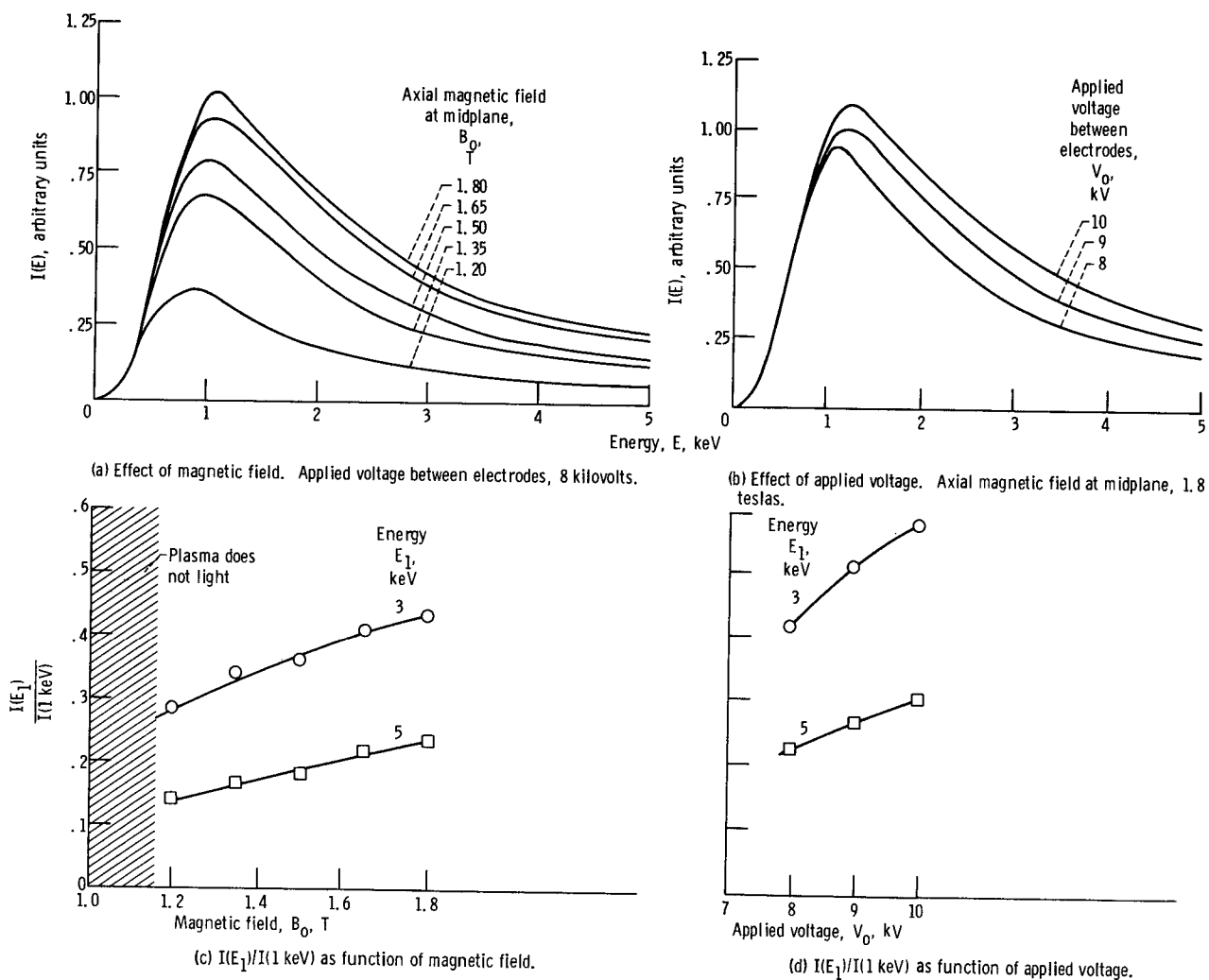


Figure 7. - Parametric variations of neutral particle energy analyzer spectra $I(E)$ with applied voltage and axial magnetic field. Centerline sighting for hydrogen.

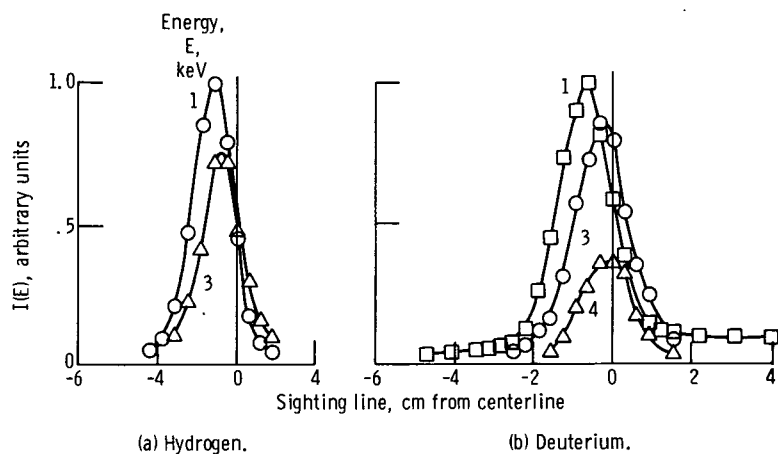


Figure 8. - Neutral particle energy current $I(E)$ as function of sighting position.

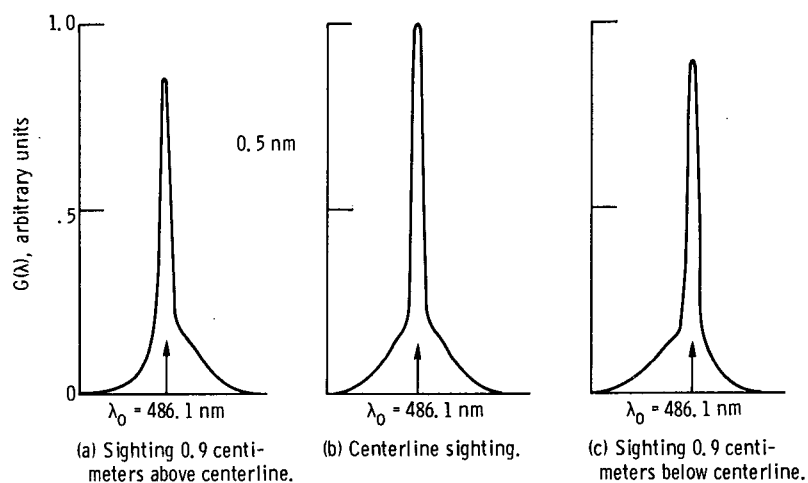


Figure 9. - Typical $H\beta$ spectra. Applied voltage between electrodes, 8 kilovolts; axial magnetic field at midplane, 1.35 teslas.

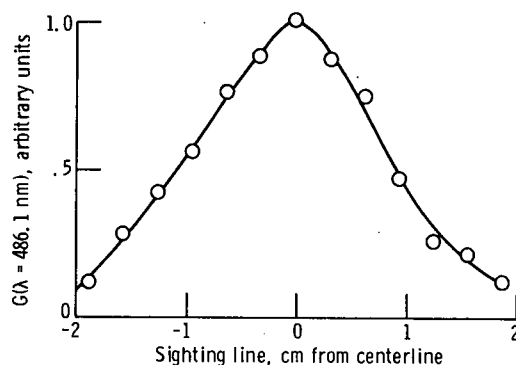


Figure 10. - $G(\lambda = 486.1 \text{ nm})$ as function of sighting position.